Scientific Research Publishing

Open Journal of Applied Sciences, 2025, 15(3), 564-572
https://www.scirp.org/journal/ojapps
ISSN Online: 2165-3925
ISSN Print: 2165-3917

Finite Element Analysis of a New Type of Self-Insulating Concrete Masonry Wall System

Abu-Bakre A. Elamin[1], Bashir H. Osman[2]

[1]Civil Engineering Department, College of Engineering, University of Technology, Khartoum, Sudan
[2]Civil Engineering Department, College of Engineering, University of Sinnar, Sinnar, Sudan
Email: abubakre55@yahoo.com, bashir00@yahoo.com

How to cite this paper: Elamin, A.-B.A. and Osman, B.H. (2025) Finite Element Analysis of a New Type of Self-Insulating Concrete Masonry Wall System. *Open Journal of Applied Sciences*, **15**, 564-572.
https://doi.org/10.4236/ojapps.2025.153036

Received: January 30, 2025
Accepted: March 7, 2025
Published: March 10, 2025

Abstract

The use of thermal insulation materials in the production of masonry is one of the most effective ways of using green building technology. An evaluation of key design and wall parameters which affect the performance of the self-insulating concrete masonry shear walls (SCMSW) is presented. Numerical models using simplified micro modeling techniques were developed to predict the behavior of the building. Performance is evaluated with respect to predicted load capacities, drift, displacement ductility, plastic hinge length, amount of energy dissipation and value of equivalent hysteretic damping. The FE results by using ABAQUS were also compared to results obtained by an experimental program to gain a better understanding of how the parameters influence wall behavior, and the results were in accordance. It was concluded that the proposed models can be used to deduct the general behavior of grouted specimens. Finally, an example of an eighteen-story building under an earthquake excitation was provided to provide a practical application of self-insulating concrete masonry shear walls.

Keywords

Concrete, Masonry, Self-Insulating, ABAQUS, Wall

1. Introduction

Design and selection of building materials and their components are an efficient way to reduce energy consumption. Thus, enveloping buildings with thermal insulation materials is one of the most effective ways to reduce energy consumption [1] [2]. Several studies have been carried out on this subject, and it is thought that the building type, shape, construction materials, insulation materials, and costs affect the thickness of an insulator [3]-[7].

In general, external insulation methods are preferred around the world. However, the use of insulation blocks composed of Expanded Polystyrene Foam (EPS), which is an alternative to building external insulation, has become more widespread with the intention of thermal insulation. EPS used for heat and sound insulation or packaging is composed of small, white and interconnected beads and exhibits superior engineering properties due to its structure such as lightweight, versatile, energy efficient, and cost effective. Therefore, it is used as insulation material in buildings and can be molded into many shapes for different purposes [8] [9].

Most previous researches focus on light weight concrete masonry units as good thermal insulation materials in buildings because they have a lower thermal conductivity than normal weight concrete. Unfortunately, masonry units made from light weight concrete have low mechanical properties compared with normal weight concrete [10]-[14]. By inserting insulation material such as EPS into normal weight concrete with a special configuration of concrete masonry units (CMUs) leads to increase in their thermal resistance without an effect of their mechanical performance [15].

2. Modelling Verification

Firstly, the FE using Abaqus software was verified with experimental results which published by Abu-Bakre *et al.* (2016, 2017) [16] [17] and the details of the tested specimens are shown in **Table 1**. The comparison of FE model results with the experimental results was aimed to ensure that the material and elements properties, and convergence criteria are suitable to model the behavior of the wall and that the simulation process is correct. Therefore, the walls which tested experimentally were simulated for verification study.

Table 1. Self-insulated concrete masonry shear wall specimens' details [16] [17].

Wall	Height (mm)	Length (mm)	Thickness (mm)	Aspect ratio	Reinforcement				Axial stress (N/mm^2)
					vertical	horizontal	ρ_v%	ρ_h%	
SW1	1590	1590	240	1.0	Ø16@200 mm	Ø8@200 mm	0.46	0.115	0.00
SW2	3190	1590	240	2.0	Ø16@200 mm	Ø8@200 mm	0.46	0.115	0.50
SW3	3190	1590	240	2.0	Ø16@200 mm	Ø8@200 mm	0.46	0.115	1.0
SW4	5780	1590	240	3.6	Ø16@200 mm	Ø8@200 mm	0.46	0.115	1.0
SW5	5780	1590	240	3.6	Ø20@200 mm	Ø8@200 mm	0.718	0.115	1.0
SW6	5780	2190	240	2.6	Ø16@200 mm	Ø8@200 mm	0.667	0.115	1.0

As shown in **Table 2**, there was good relationship between the FE and experimental load-deflection curves. This confirmed the validity of the settled FE models and reliability of the FE analysis.

3. Finite Element Analysis

The finite element method (FEM) is one of the powerful tools for modeling a structure with a very complicated geometry and materials. There are many strategies as shown in Figure 1 to model masonry structure with FEM, which includes macro and micro modeling. The macro model is based on the assumption of homogenous materials, and the mortar joints and units can be smeared into one isotropic or anisotropic material. This procedure may be preferred for the analysis of large masonry structures due to the reduced time and memory requirements as well as a user-friendly mesh generation. In addition, this type of modeling is most valuable when a compromise between accuracy and efficiency is needed [18] [19].

Finite element analysis was performed using Abaqus software to validate the experimental results of SCMSW specimens.

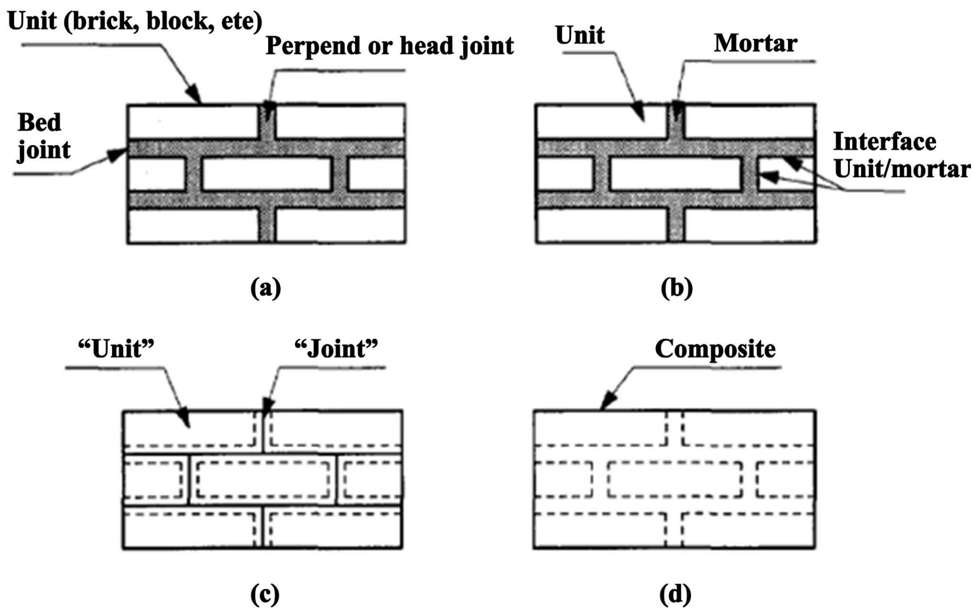

Figure 1. Modeling strategies for block masonry. (a) Typical masonry sample; (b) Detailed micro modeling; (c) Simplified micro modeling; and (d) Macro modeling.

3.1. Material Constitutive Models

The damage plasticity model from the Abaqus software was applied to simulate the concrete constitutive law. Using the same methods described in chapter three. The masonry compressive strength obtained was extracted from compression test data for masonry prism, and Poisson's ratio was taken as 0.2. The concrete material used in the foundation and loading beams was obtained from concrete compression test, and Poisson's ratio was taken as 0.2.

The "plasticity" model from Abaqus software was adopted to simulate the reinforcement law. The stress-strain curve is plotted in Figure 2. Each stress-strain curve, made up of two linear portions, represents the character of a bare mild steel bar; where the modulus E_s is the elastic modulus of the reinforcement and the modulus E' is the deformation modulus at the strain hardening stage, $E' = 0.01E_s$. The test yield strength and elastic modulus of the reinforcement were adopted in chapter five, and Poisson's ratio was taken as 0.3.

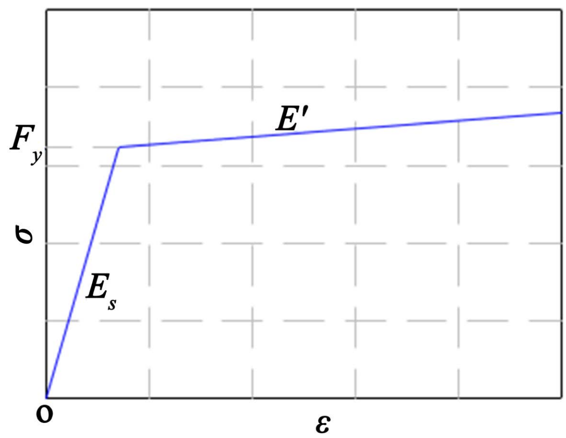

Figure 2. Stress-strain curve of reinforcement.

3.2. Finite Element Analysis Model

Solid element C3D8R was used for concrete and masonry wall, and truss element T3D2 was used for reinforcement. The interface model between masonry wall and loading beam was composed by contact in the lateral axis and stick-slip along the tangential axis. The "hard contact" model was adopted for the contact on the lateral axis and the "Coulomb friction" model for the stick-slip along the tangential axis. The friction coefficient was taken as 0.7 according to the code GB5003-2011 [20]. Reinforcements were all embedded in the concrete. The bottom of the base was fixed rigidly. A vertically distributed load was applied to the top of the loading beam first and kept constant. Then, horizontal displacement was applied to a coupling node in the middle plane of the loading beam. A typical finite element analysis model of SW2 is shown in Figure 3.

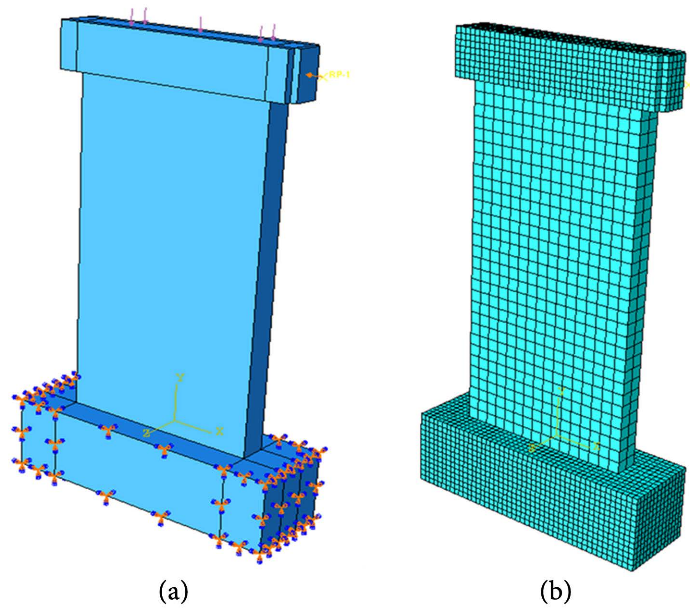

Figure 3. Finite element analysis model of SW2: (a) Loading and boundary conditions (BCs); and (b) Element mesh.

4. Finite Element Simulation Results and Analysis

Figure 4 shows the Von Mises stresses distribution in SW3 specimen at maximum load. While Table 2 shows the maximum load values measured by experiment and predicted by finite element software Abaqus. A good agreement is shown between the numerical and experimental results.

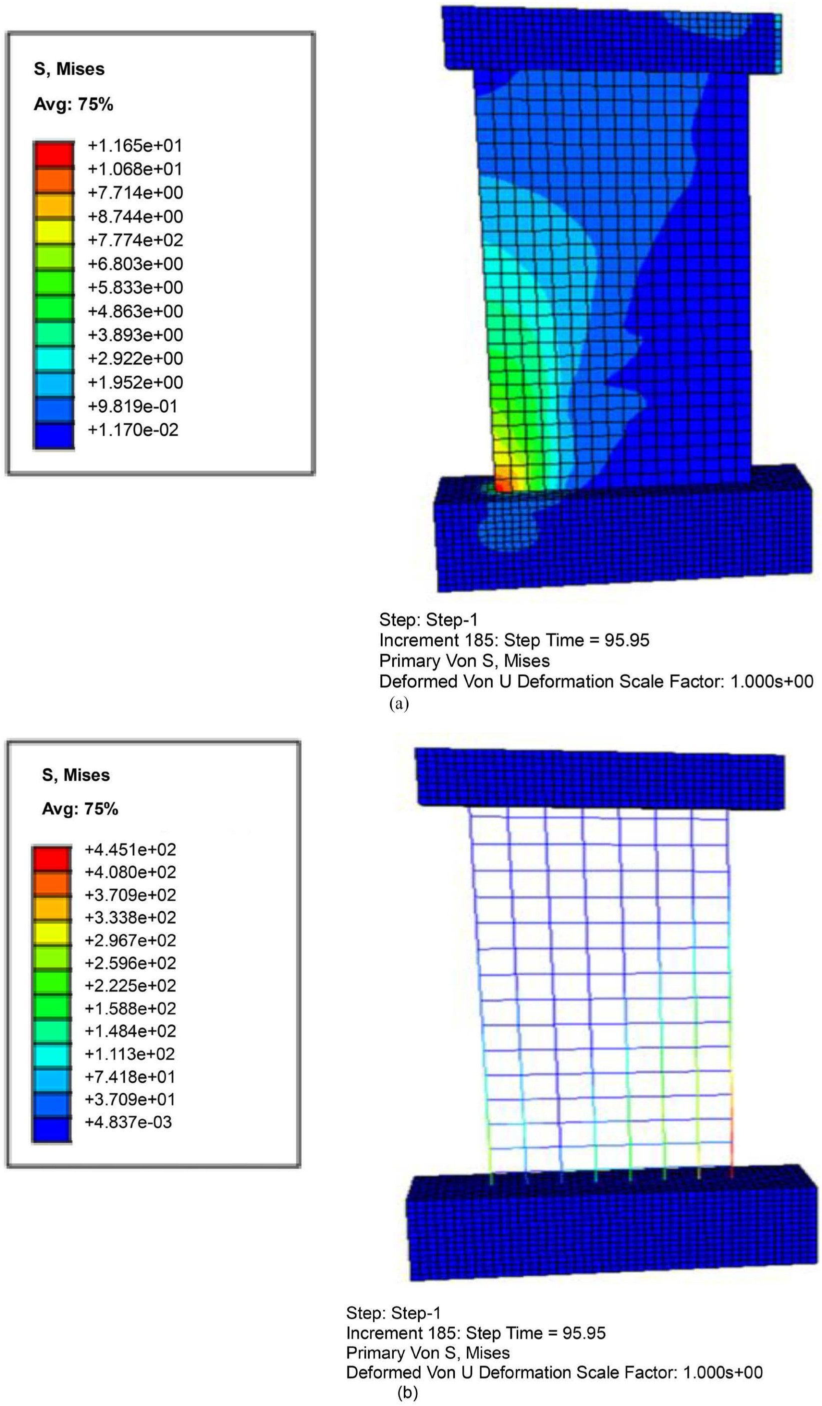

Figure 4. SW3 F.E. results: (a) Von Mises stresses distribution at wall reinforcement; and (b) Von Mises stresses at masonry wall.

Table 2. Comparison of predicted load by F.E and experimental capacities.

Wall	Aspect ratio	Axial stress (N/mm²)	Vertical reinforcement	F.E. maximum load (kN)	Average observed capacity (kN)	Ratio of observed capacity to F.E. results
SW1	1.0	0.0	Ø16@200 mm	290	327	1.13
SW2	2.0	0.5	Ø16@200 mm	194.4	159	0.82
SW3	2.0	1.0	Ø16@200 mm	208.6	209.7	0.95
SW4	3.6	1.0	Ø16@200 mm	125.4	112.6	1.0
SW5	3.6	1.0	Ø20@200 mm	154.5	146.3	0.95
SW6	2.6	1.0	Ø16@200 mm	320	359.6	1.12

5. Design Example

The 18-storey residential building as shown in Figure 5 is composed of self-insulated concrete masonry shear walls was analyzed by using ETABS (v9.5.0) software. The building is designed for the seismic intensity of 8 according to Chinese standard.

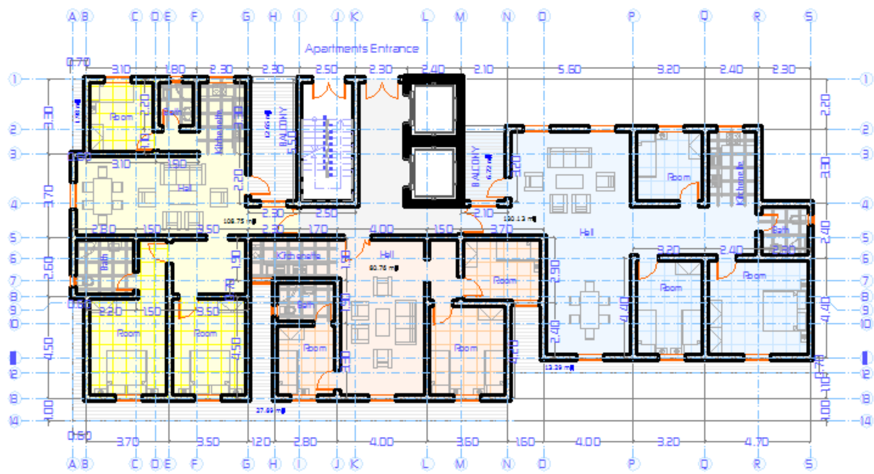

(a)

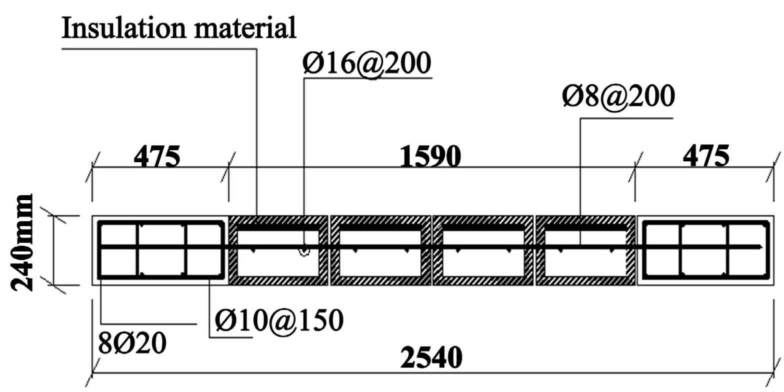

(b)

Figure 5. Model example geometry (a) Typical architecture floor plan (b) reinforcement details.

The structural model was generated using ETABS software to give a practical application for the self-insulating concrete masonry shear walls in general engineering practice. Self-weight of structural elements, finishing load of 3 kN/m^2 and live load of 2 kN/m^2, act at each floor and at roof level were applied to the structural model. The maximum horizontal displacements for X and Y direction under earthquake excitations were found 15 and 30 mm, respectively. Moreover, the first mode shape time period is 0.97 second, while the second and third mode shapes time period are 0.14 and 0.07 second, respectively. According to this example the new type of self-insulating concrete masonry shear walls can be used in areas have seismic intensity of 8 or less and it is application valid until 18-storey height building. The FE model and shape of the studied Building are shown in **Figure 6**.

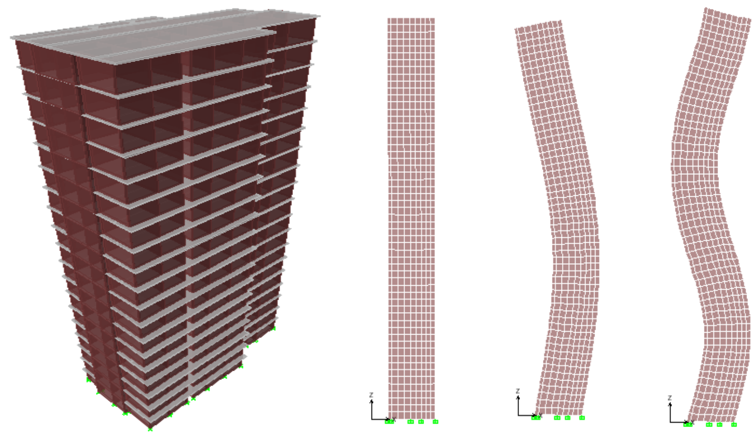

(a) (b)

Figure 6. (a) Rendered view of the model (b) Building mode shapes.

6. Conclusion

This paper evaluated the effects that the height-to-length aspect ratio, axial compressive stress, and reinforcement ratio have on the behavior of self-insulating concrete masonry shear walls under in-plane cyclic loading. SCMSW specimens' performance was evaluated based on a comparison of predicted vs. actual load capacity, drift capacity, displacement ductility, height of plasticity, equivalent plastic hinge length, amount of energy dissipated, and value of equivalent hysteretic damping. Moreover, finite element results obtained from the Abaqus program were compared to those obtained experimentally. Finally, a design example of the 18-storey building under an earthquake excitation was provided to give a practical application of the self-insulating concrete masonry shear walls.

Conflicts of Interest

The authors declare no conflicts of interest regarding the publication of this paper.

References

[1] Ghrab-Morcos, N. (2005) CHEOPS: A Simplified Tool for Thermal Assessment of

Mediterranean Residential Buildings in Hot and Cold Seasons. *Energy and Buildings*, **37**, 651-662. https://doi.org/10.1016/j.enbuild.2004.09.020

[2] Mohsen, M.S. and Akash, B.A. (2001) Some Prospects of Energy Savings in Buildings. *Energy Conversion and Management*, **42**, 1307-1315. https://doi.org/10.1016/s0196-8904(00)00140-0

[3] Al-Homoud, D.M.S. (2005) Performance Characteristics and Practical Applications of Common Building Thermal Insulation Materials. *Building and Environment*, **40**, 353-366. https://doi.org/10.1016/j.buildenv.2004.05.013

[4] Ansari, F.A., Mokhtar, A.S., Abbas, K.A. and Adam, N.M. (2005) A Simple Approach for Building Cooling Load Estimation. *American Journal of Environmental Sciences*, **1**, 209-212. https://doi.org/10.3844/ajessp.2005.209.212

[5] Al-Khawaja, M.J. (2004) Determination and Selecting the Optimum Thickness of Insulation for Buildings in Hot Countries by Accounting for Solar Radiation. *Applied Thermal Engineering*, **24**, 2601-2610. https://doi.org/10.1016/j.applthermaleng.2004.03.019

[6] Yu, J., Yang, C., Tian, L. and Liao, D. (2009) A Study on Optimum Insulation Thicknesses of External Walls in Hot Summer and Cold Winter Zone of China. *Applied Energy*, **86**, 2520-2529. https://doi.org/10.1016/j.apenergy.2009.03.010

[7] Osman, B.H. and Chen, Z. (2018) Experimental Studies on the Behaviors of New Energy-Saving Concrete Self-Insulating Load-Bearing Block Wall under Low-Cycle Cyclic Loading. *Advances in Materials Science and Engineering*, **2018**, Article ID: 4214532. https://doi.org/10.1155/2018/4214532

[8] Demirel, B. (2013) Optimization of the Composite Brick Composed of Expanded Polystyrene and Pumice Blocks. *Construction and Building Materials*, **40**, 306-313. https://doi.org/10.1016/j.conbuildmat.2012.11.008

[9] Osman, B.H., Chen, Z.F. and Carrol, A. (2024) Optimization and Design of Mixture Ratio and Basic Properties for New Energy-Saving Concrete Self-Insulation Block. *Journal of the Croatian Association of Civil Engineers*, **76**, 119-137. https://doi.org/10.14256/JCE.3821.2023

[10] Ding, X.Y., Luo, Y.L., Chen, Z.F. and Xu, M. (2014) Self-insulation Concrete Block Design and Optimized Design Based on Thermal and Mechanical Properties in Severe Cold Zones. *Advanced Materials Research*, **1051**, 730-736. https://doi.org/10.4028/www.scientific.net/amr.1051.730

[11] Javidan, F. (2013) Shape Optimization of Hollow Concrete Blocks Using the Lattice Discrete Particle Model. *Iranica Journal of Energy & Environment*, **4**, 243-250. https://doi.org/10.5829/idosi.ijee.2013.04.03.10

[12] Asjodi, A.H., Saeidi, S., Dolatshahi, K.M. and Burton, H.V. (2024) Quantifying Hybrid Failure Modes of Unreinforced Masonry Walls through Experimental Data Analysis. *Journal of Structural Engineering*, **150**, Article ID: 04024155. https://doi.org/10.1061/jsendh.steng-13028

[13] del Coz Díaz, J.J., Nieto, P.J.G., Rodríguez, A.M., Martínez-Luengas, A.L. and Biempica, C.B. (2006) Non-Linear Thermal Analysis of Light Concrete Hollow Brick Walls by the Finite Element Method and Experimental Validation. *Applied Thermal Engineering*, **26**, 777-786. https://doi.org/10.1016/j.applthermaleng.2005.10.012

[14] Al-Jabri, K.S., Hago, A.W., Al-Nuaimi, A.S. and Al-Saidy, A.H. (2005) Concrete Blocks for Thermal Insulation in Hot Climate. *Cement and Concrete Research*, **35**, 1472-1479. https://doi.org/10.1016/j.cemconres.2004.08.018

[15] Christine, B. (2004) Masonry Design and Detailing: For Architects and Contractors.

McGraw-Hill.

[16] Abdelmoneim Elamin Mohamad, A. and Chen, Z. (2016) Experimental and Numerical Analysis of the Compressive and Shear Behavior for a New Type of Self-Insulating Concrete Masonry System. *Applied Sciences*, **6**, Article 245. https://doi.org/10.3390/app6090245

[17] Elamin Mohamad, A.B.A. and Chen, Z.F. (2017) Experimental Studies on Behavior of a New Type of Self-Insulating Concrete Masonry Shear Walls Under In-Plane Cyclic Loading. *Applied Sciences*, **7**, Article 463.

[18] Lourenco, P.B. (1996) Computational Strategies for Masonry Structures. Delft University Press.

[19] Marques, R. and Lourenço, P.B. (2011) Possibilities and Comparison of Structural Component Models for the Seismic Assessment of Modern Unreinforced Masonry Buildings. *Computers & Structures*, **89**, 2079-2091. https://doi.org/10.1016/j.compstruc.2011.05.021

[20] Ministry of Housing and Urban-Rural Development of the People's Republic of China (2011) Code for Design of Masonry Structures GB50003-2011. China Architecture Building Press.